KAWASAKI STEEL TECHNICAL REPORT
No.6 (September 1982)

Effects of Chemical Composition and Structure of Hot Rolled High Strength Steel Sheets on the Formability of Flash Butt Welded Joints

Masatoshi Shinozaki, Toshiyuki Kato, Toshio Irie, Hiroshi Hashimoto

Synopsis :
To clarify the factors required of high strength steels for wheel rim use, formability of flash butt welded joints in three types of hot rolled high strength sheet steels, i.e., solid solution hardened steel, precipitation hardened steel and dual phase steel was investigated. Formability in stretch-flanging is closely related to changes in the hardness and microstructure of the weld. It is impaired by localized fracture due to softening at the heat affected zone or weld interface in dual phase steels and precipitation hardened steels having low alloy content. To avoid softening precipitation hardened steel, the carbon equivalent should be raised in proportion to tensile strength in the newly proposed equation for Ceq [FBW]. Formability in bending is deteriorated by two types of defects, i.e., penetrator crack and hook crack. The former is caused by oxides generated at the weld interface during welding. It can be suppressed by controlling Si and Mn contents to maintain the Mn/Si ratio in an adequate range of 4 to 23. Hook crack can be suppressed by lowering the amount of sulfide inclusions.

The body can be viewed from the next page.

Effects of Chemical Composition and Structure of Hot Rolled High Strength Steel Sheets on the Formability of Flash Butt Welded Joints*

Masatoshi SHINOZAKI** Toshiyuki KATO** Toshio IRIE**
Hiroshi HASHIMOTO***

To clarify the factors required of high strength steels for wheel rim use, formability of flash butt welded joints in three types of hot rolled high strength sheet steels, i.e., solid solution hardened steel, precipitation hardened steel and dual phase steel was investigated.

Formability in stretch-flanging is closely related to changes in the hardness and microstructure of the weld. It is impaired by localized fracture due to softening at the heat affected zone or weld interface in dual phase steels and precipitation hardened steels having low alloy content. To avoid softening in precipitation hardened steel, the carbon equivalent should be raised in proportion to tensile strength in the newly proposed equation for C_{eq} [FBW].

Formability in bending is deteriorated by two types of defects, i.e., penetrator crack and hook crack. The former is caused by oxides generated at the weld interface during welding. It can be suppressed by controlling Si and Mn contents to maintain the Mn/Si ratio in an adequate range of 4 to 23. Hook crack can be suppressed by lowering the amount of sulfide inclusions.

1 Introduction

As automobile parts requiring weight reduction in the Japanese auto industry, attention was focused first on the car bodies mainly made of cold rolled sheet steels and recently on wheels and drivability related parts using hot rolled sheet steels. Hot rolled parts, because of their greater sheet thickness in general, have a margin in stiffness, permitting a significant gage-reduction effect. A wheel consists of a rim and a disk. The disk is press-formed, but the manufacturing processes of the rim comprise flash butt welding of hoop and subsequent roll forming. At roll forming, the hoop is subjected to flaring and bending. Flaring is a kind of stretch-flanging, and the welded joint poor in stretch-flangeability causes fracture or necking in the flaring process. Welded joints poor in bendability generate pinholes and microcracks, resulting in air leaks on tubeless tires, although rim forming is possible. The cold formability of welded joints of high strength sheet steels is inferior to that of mild steel, and thus the development of high strength sheet steels which are not liable to generate the above-mentioned defects is strongly desired. Up to now, it has been clarified to some extent that the hardening mechanism and formability of high strength sheet steels are affected by the chemical composition and production method, but the relation between the cold formability of the flash butt welded joint and the hardening mechanism of sheet steel or its chemical composition has not systematically been investigated and reported, although some efforts have been made to clarify the relationship in part[1-4].

The present report aims at clarifying the chemical composition conditions necessary for hot rolled high strength sheet steel for wheel rim use, and gives the results of investigation on the cold formability of flash butt welded joints of various types of hot rolled sheet steels.

* Originally published in *Tetsu-to-Hagané*, **68** (1982) 9, p. 214
** Research Laboratories
*** Mizushima Works

Table 1 Chemical composition of steels used

(Wt%)

C	Si	Mn	P	S	Al	Cr	Nb, Ti, V	Mo	B
0.04 ~ 0.15	0.21 ~ 1.1	0.2 ~ 2.5	≃0.02	0.001 ~ 0.02	0.001 ~ 0.02	0.03 ~ 1.0	Tr-0.06	Tr-0.2	Tr-0.005

Table 2 Conditions of flash-butt welding

Size of specimen	t×50×90 mm³
Secondary voltage	4.8 V
Curve of platen travel	Parabola
Flash-off	13 mm
Flashing time	4.0 s
Upsetting current time	0.2 s
Upsetting force	Exerted by compressed air
Upset distance	5 mm

2 Materials Used and Experimental Procedure

Materials used are three types of hot rolled high strength sheet steels, i.e., solid solution hardened steel, dual phase steel, and precipitation hardened steel. Mild steel was used for comparison. **Table 1** shows the range of their chemical compositions. The range of their thickness is within 2.6 to 2.9 mm, and their tensile strength is within the range of 34 to 65 kgf/mm².

The welder used for the experiment is a compressed-air type flash butt welder, and the sample was moved by the action of a cam. The welding conditions employed in the experiment are shown in **Table 2**. The stretch-flangeability was evaluated by its elongation using the side-bend tester[5] shown in **Fig. 1**. The test piece with the as-sheared edge was bent by the punch as illustrated in **Fig 1(a)**. Side-bend elongation, SEl (%), is expressed by SEl. $= 100 \times (L - L_0)/L_0$, where L_0 is gage length (50 mm), and L is the length between two scratched lines at the onset of failure.

When the welded joint was to be tested, beads were removed by grinding and then the weld line was aligned to the center of the gage length. A bend test of the welded joint illustrated in **Fig. 2** was also performed on the test piece, and its bendability was evaluated by the occurrence ratio of the defects. In the bend test, both surfaces of the entire welded joint were ground after the beads were removed, and the test piece was bent by pressing it with a punch into the die having an angle of 40°. Defects generated by the bend test include penetrator crack and hook crack, and these two types of cracks occurred on the weld line and on the portion along the weld line, respectively.

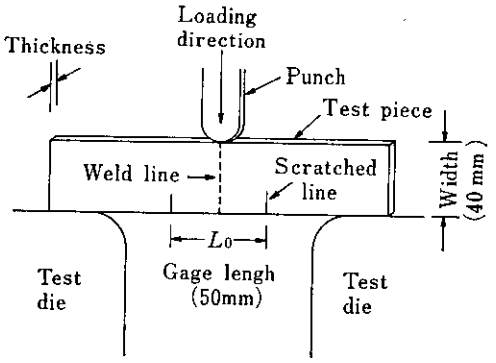

(a) Side-bend testing tool

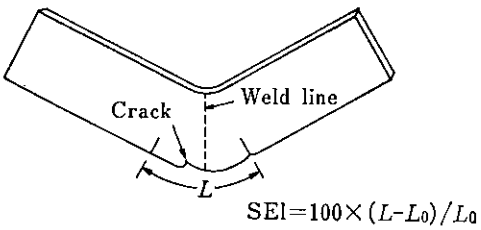

(b) Specimen deformed

Fig. 1 Method of side-bend test

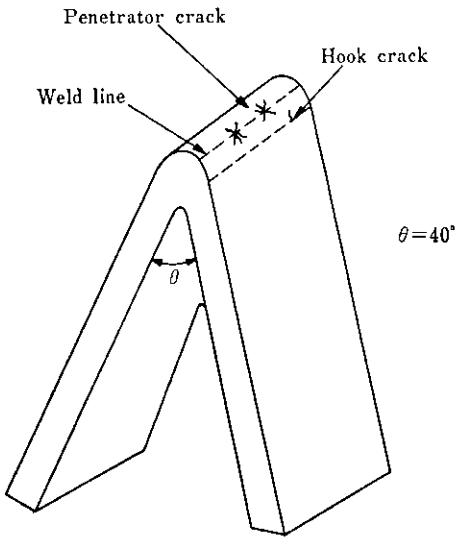

Fig. 2 Method of bend test and defects in welded joint

3 Results of Experiments

3.1 Stretch-flangeability of Sheets

Fig. 3 shows the relation between the side-bend elongation and TS. Steel sheets for the rim must have excellent stretch-flangeability in the first place, but the side-bend elongation of the sheet drops as the TS value becomes higher. This trend, however, is dependent on S content, and steel sheets with lower S content show greater side-bend elongation, TS being equal. When the S content is 30 ppm and under or over 30 ppm, the following regression equations are obtained, respectively, between the side-bend elongation, SEl. (%), and TS (kgf/mm²):

$$\underline{S} \leqq 30 \text{ ppm}: \text{SEl} = -2.0\,\text{TS} + 159 \quad \cdots\cdot(1)$$

$$\underline{S} > 30 \text{ ppm}: \text{SEl} = -1.4\,\text{TS} + 113 \quad \cdots\cdot(2)$$

3.2 Stretch-flangeability of Welded Joint

Fig. 4 shows the relation between the SEl of the welded joint and that of the sheet. The former is smaller than the latter, and this difference varies depending on the types of steel, as follows:

(1) The SEl value of solid solution hardened steel drops by a maximum of 20% owing to welding, but still retains a higher value, and the locations of crack all lay at the base metal.

(2) Dual phase steel has cracked at the HAZ (heat-affected zone) and its SEl is small.

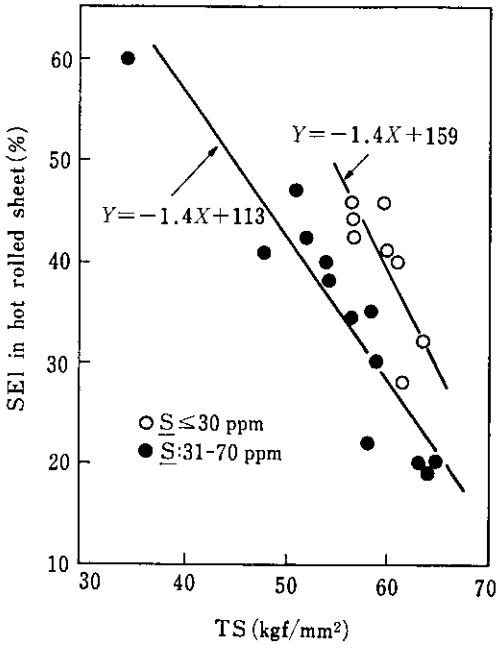

Fig. 3 Relation between tensile strength and SEl in hot rolled sheets

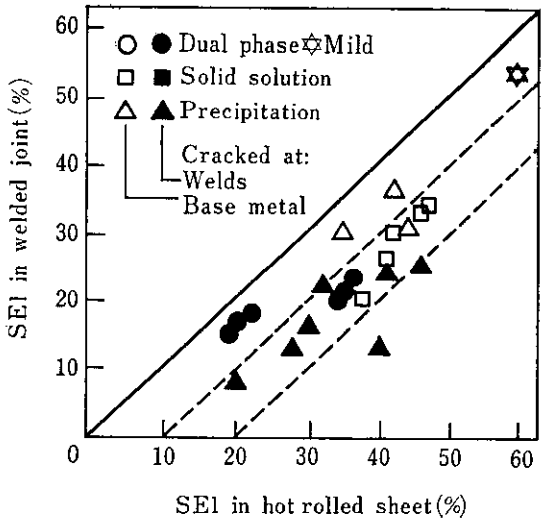

Fig. 4 Relation between SEl in hot rolled sheets and that in flash-butt welded joints

(3) Precipitation hardened steel cracks at the base metal or at the weld (weld interface or HAZ), and the precipitation hardened steel which cracks at the weld has smaller SEl. The dimensions and shapes of rims have been determined by the JASO Standard, and the stretch-flanging at time of rim formation is 20 to 25%. Therefore, SEl of the welded joint must be 25% and over.

3.3 Microstructure and Hardness Traverse of Weld

Photos 1 to **5** show changes in microstructure of welds and their hardness traverse. As an etchant, Nital was used for mild steel and the DP etchant (2% sodium metabisulfite + 4% picral)[6] was used for high strength steel in order to ascertain the existence of martensite. The portion which appears white owing to the DP etchant is martensite.

(1) Mild steel
As shown in **Photo 1**, the weld structure is more or less the same as the base metal structure (ferrite + pearlite). The hardness traverse of mild steel indicates that the weld interface is slightly hardened but shows a nearly flat profile, and the crack position in the side-bend test lies at the base metal.

(2) Solid solution hardened steel
As shown in **Photo 2**, the weld interface shows a bainite structure including some quantity of martensite, and at a position 2 to 3 mm away from the weld interface, some quantity of cementite is observed in addition to the ferrite and martensite, all of which then turn into the base metal sturcture of ferrite + pearlite. The crack position in the side-bend test is at the base metal.

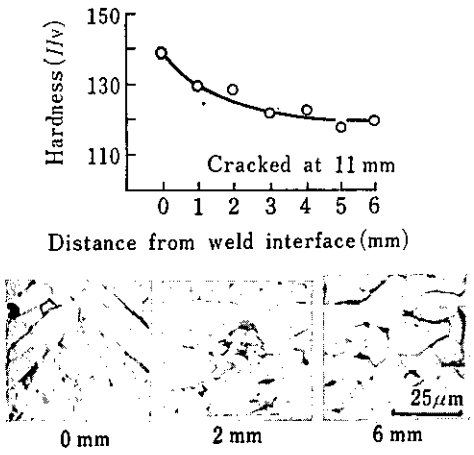

Photo 1 Microstructures (nital etching) and hardness traverse across welds in mild steel (0.08%C-0.003%Si-0.3%Mn, Ts: 34 kgf/mm²)

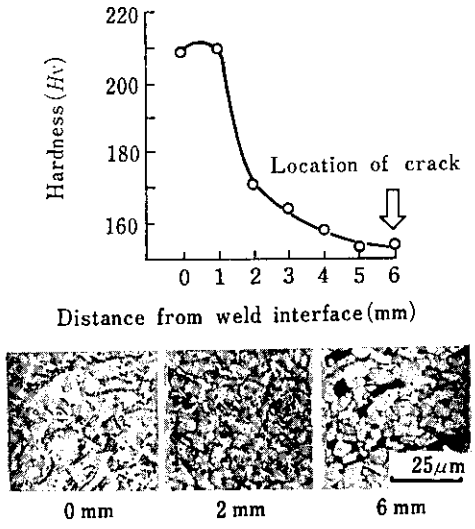

Photo 2 Microstructures (DP etching) and hardness traverse across welds in solid solution hardened steel (0.066%C-0.52%Si-1.78%Mn, TS: 52 kgf/mm²)

(3) Dual phase steel

As shown in **Photo 3**, the weld interface comprises a "bainite + martensite" structure, and at the position 2 to 3 mm away from the weld interface, a "ferrite + martensite" structure is observed, and the hardness of these two structures is higher than that of the base metal. The crack position is 4 to 5 mm away from the weld interface, and at this crack position, martensite is tempered (white phase has decreased or disappeared), and its hardness has dropped below that of the base metal. At a position 8 to 10 mm away from the weld interface lies the base metal structure (ferrite + martensite).

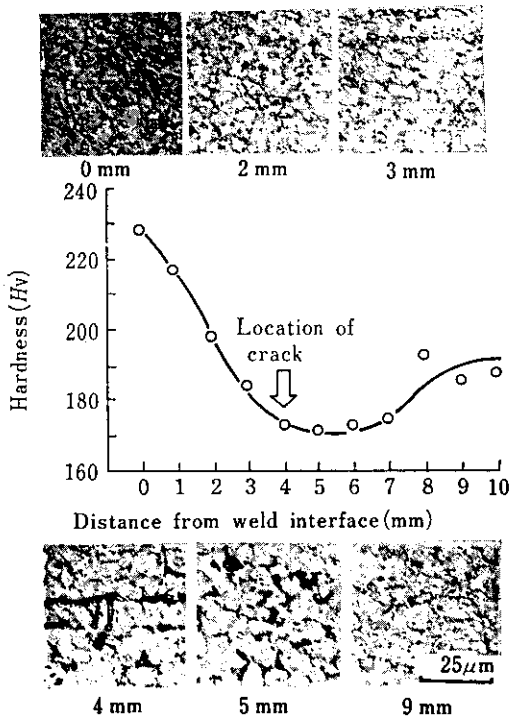

Photo 3 Microstructures (DP etching) and hardness traverse across welds in dual phase steel (0.063%C-0.52%Si-1.79%Mn, TS: 53 kgf/mm²)

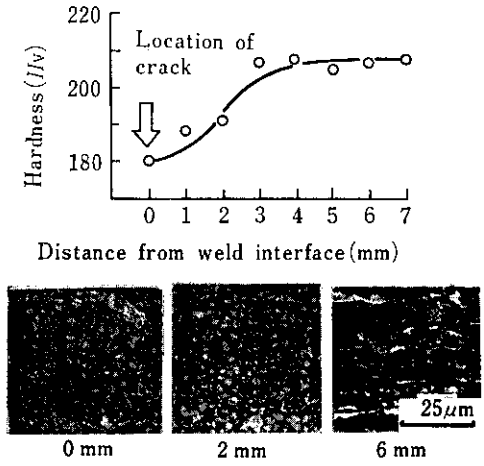

Photo 4 Microstructures (DP etching) and hardness traverse across welds in precipitation hardened steel(I) (0.084%C-0.05%Si-1.07%Mn-0.052%Ti, TS: 64 kgf/mm²)

(4) Precipitation hardened steel (I)

As shown in **Photo 4**, the crack position lies at the weld interface, ferrite bands are observed here

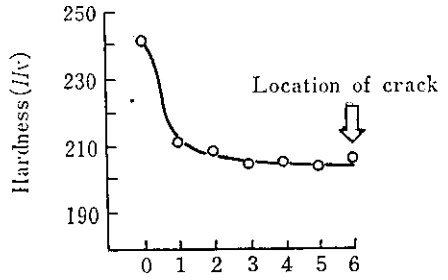

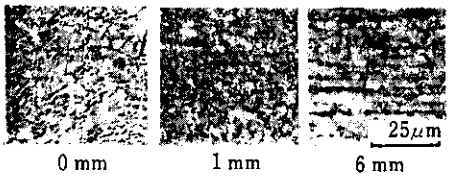

Photo 5 Microstructures (DP etching) and hardness traverse across welds in precipitation hardened steel(II) (0.097%C-0.35%Si-1.44%Mn-0.044%Nb, TS: 61 kgf/mm²)

and hardness is the lowest. The position 1 mm away from the weld interface consists of a "ferrite + bainite" structure, and the position 2 mm away consists of a normalized structure of ferrite with fine grains. The hardness of these two structures is slightly lower than that of the base metal. The position 3 mm and over away from the weld interface consists of the base metal structure (ferrite + pearlite), and no martensite is observed at any position on this steel.

(5) Precipitation hardened steel (II)
As shown in **Photo 5**, the weld interface shows a bainite structure containing some quantity of martensite, and the position 1 to 2 mm away from the weld interface comprises a "ferrite + martensite" structure, these two portions having hardness higher than that of the base metal. The position 3 mm and over away from the weld interface is the base metal structure (ferrite + pearlite), and the crack position lies at the base metal.

As shown above, the crack positions in the side-bend test coincide with the softened portions, and the hardness traverse shows good correspondence to changes in structures.

3.4 Bendability of Welded Joint

Of the defects generated by the bend test of welded joints, the penetrator crack shows a sectional shape as shown in **Photo 6**, and there is a difference as shown in the **Photo 7** between its fracture surface and the fracture surface after tensile test of a soundly welded

Photo 6 Cross section of penetrator crack

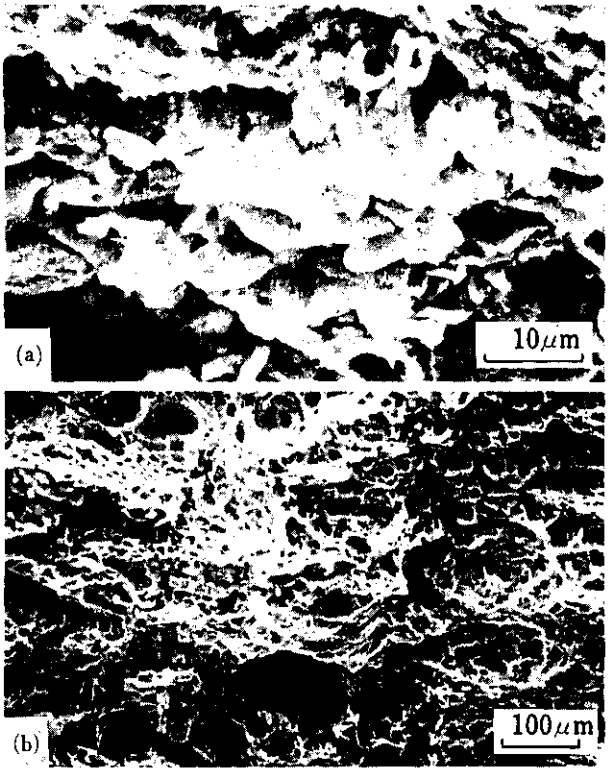

Photo 7 Scanning electron micrographs of fractured surface at weld interface
(a) penetrator crack
(b) sound weld interface

joint. The soundly welded joint shows dimples, whereas the fracture surface of the penetrator crack shows a cluster-shaped substance, from which Fe, Si, Mn, Al and Ca or Ti and O were detected when analyzed by EPMA. Therefore, the main body of the penetrator crack comprises oxides generated during welding, and to prevent their generation, it is desirable that the elements which are liable to form oxides be small in quantity. The penetrator cracking ratio in

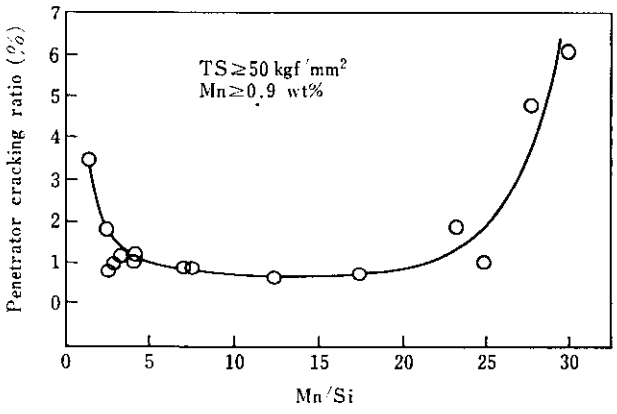

Fig. 5 Relation between penetrator cracking occurrence ratio and Mn/Si

high strength sheet steels having a TS value of 50 kgf/mm² and over and containing 0.9 wt% Mn is rearranged into the Mn/Si ratio as shown in **Fig. 5**, and it is found that when this ratio is 4 to 23, the penetrator cracking ratio is lower, but no clear relation is observed between this cracking ratio and the individual quantities of Mn, Si and other elements. Incidentally, this penetrator cracking ratio is equal to the value of the total crack length divided by the weld line.

On the welded joint which has generated a hook crack, elongated inclusions and clustered inclusions are observed along the metal flow, and the hook crack also has propagated along the metal flow. Therefore, it can be understood that the hook crack has been caused by inclusions in the base metal. According to the EPMA analysis, the elongated inclusions mainly consist of MnS and SiO_2. The relation between the S content and the hook cracking ratio (ratio of number of cracked specimens to number of total specimens) is shown in **Fig. 6**, and if the S content exceeds 0.005 wt% the hook cracking ratio rises. Consequently, reduction in S content is effective in suppressing hook

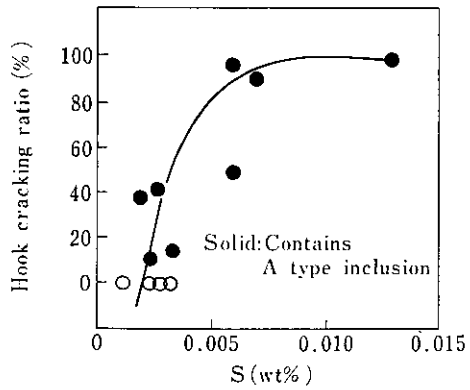

Fig. 6 Effect of S content on hook cracking ratio

crack and improving the stretch-flangeability of the sheet (see **Fig. 3**).

4 Discussion

As mentioned in Par. 3.3, the crack position in the side-bend test coincides with the softened zone, and when there is a softened zone, fracture or necking occurs during rim forming; therefore, dual phase steel and precipitation hardened steel (I) are not suitable as materials for rims. Solid solution hardened steel does not generate a softened zone, but large amounts of Mn and Si must be added in order to obtain a TS value of 55 kgf/mm² and over, thereby causing an undesirable increase in production cost. Consequently, precipitation hardened steel (II) whose weld does not soften is most suitable for the rim-making material of TS 55 kgf/mm² and over.

Next, discussion will be made on the reasons why the precipitation hardened steel (I) softened at the weld interface, while precipitation hardened steel (II) hardened there.

The authors have ascertained by experiments that the hardness of the weld interface hardly changes depending upon the magnitude of the heat input. This indicates that since the weld interface is once heated to the melting point and over and then cooled down from the solidification stage at practically the same cooling rate, it is considered that the weld interfaces produce virtually the same structure regardless of the magnitude of the heat input, chemical compositions being equal. This cooling rate is primarily governed by the thermal conductivity of the steel sheet, unless the weld is intentionally subjected to heating and cooling treatment, and this is a value inherent to the steel sheet concerned. Therefore, if the relation between the chemical composition and hardness of the weld interface is obtained from various kinds of steels, it may become possible to explain the softening or hardening of the weld interface of precipitation hardened steel.

Therefore, hardness values at weld interfaces of mild steels, solid solution hardened steels and precipitation hardened steels, 23 kinds in all, were measured as shown in **Table 3** and the effects of chemical components (wt%) Vickers hardness, H_V, at weld interface were obtained by means of multiple regression calculations. The multiple regression model equation is:

$$\begin{aligned} H_V = {} & \text{Constant} + a \cdot \text{C} + b \cdot \text{Si} + c \cdot \text{Mn} \\ & + d \cdot \text{Cr} + e \cdot \text{Nb} + f \cdot \text{V} + g \cdot \text{Ti} \\ & + h \cdot \text{Mo} + i \cdot \text{B} + j \cdot \text{C} \cdot \text{Nb} \\ & + k \cdot \text{C} \cdot \text{V} + l \cdot \text{C} \cdot \text{Ti} \\ & + m \cdot \text{C} \cdot \text{Mo} + n \cdot \text{C} \cdot \text{B} \quad \cdots\cdots (3) \end{aligned}$$

Judging from the results of the quench hardenability

Table 3 Chemical composition and hardness at weld interface of steels used for multiple regression calculation

Steel	Chemical compositions (Wt%)									Hv
	C	Si	Mn	Cr	Nb	V	Ti	Mo	B	
1	0.06	0.02	0.26	0.03	–	–	–	–	–	110
2	0.08	0.02	0.30	0.03	–	–	–	–	–	140
3	0.07	1.01	1.75	0.03	–	–	–	–	–	255
4	0.09	0.50	1.50	0.03	–	–	–	–	–	225
5	0.07	0.52	1.78	0.03	–	–	–	–	–	210
6	0.07	0.53	1.55	0.03	–	–	–	–	–	204
7	0.10	0.04	1.51	0.50	–	–	–	–	–	219
8	0.10	0.22	1.99	1.02	–	–	–	–	–	295
9	0.10	0.98	1.98	0.03	0.09	–	–	–	–	274
10	0.10	0.20	1.50	0.03	0.04	–	–	–	–	214
11	0.10	0.99	1.52	0.03	–	–	0.11	–	–	258
12	0.04	0.04	1.07	0.03	–	–	0.05	–	–	192
13	0.05	0.04	1.26	0.03	–	–	0.06	–	–	190
14	0.05	0.55	1.25	0.03	–	–	0.06	–	–	215
15	0.10	0.21	1.00	0.03	–	0.04	–	–	–	183
16	0.10	0.03	0.48	0.03	–	0.10	–	–	–	169
17	0.09	0.05	1.10	0.03	0.01	–	0 05	–	–	210
18	0.07	0.04	1.15	0.03	0.01	–	0.05	–	–	210
19	0.08	0.05	1.07	0.03	0.01	–	0.05	–	–	180
20	0.10	0.35	1.44	0.03	0.04	0.05	–	–	–	241
21	0.10	0.97	1.00	0.03	–	–	–	0.19	–	215
22	0.10	0.04	1.49	0.03	–	–	–	–	0.004	219
23	0.07	0.40	1.50	0.03	–	–	–	–	0.005	200

experiment by G.T. Eldis et al.[7], 3rd-dimensional term such as "C · Nb · Ti" which is considered negligible in contribution has been excluded from the model equation. Although N also contributes to H_V, it is not included in the model equation, because it is ordinarily constant at 50 to 70 ppm.

The results of the calculations are expressed as shown by the equation for carbon equivalent C_{eq}[FBW] (wt%), then the multiple correlation coefficient is 0.96.

$$H_V = 78 \cdot 331\ C_{eq}[FBW]\ (\sigma = 18) \quad \cdots\cdots (4)$$

$$C_{eq}[FBW] = C + Si/15 + Mn/5 + Cr/9 + 7Nb(1 - 10C) + V(50C - 1)/3 + 1.3Ti(1 - 5C) + Mo(1 - 6C)/2 + 29B(11C - 1) \quad \cdots\cdots (5)$$

The relation between C_{eq}[FBW] and observed hardness is shown in **Fig. 7** which indicates comparatively good correlation. When this C_{eq}[FBW] is used in rearranging the side-bend elongation, SEl, of welded joints of mild steel, solid solution hardened steel (SS) having a TS value of about 50 kgf/mm² and precipitation hardened steel (PH) having a TS value of about 60 kgf/mm², **Fig. 8** is obtained.

The two straight lines A and B in the figure indicate the SEl values at the weld interface and are obtained by the following procedure: Namely, the relation between TS and SEl of the parent material is expressed by either eq. **(1)** or **(2)** depending upon the difference in S content, and from these equations, eq. **(4)** and the relation of TS = 3 × H_V, the SEl values (wt%) at the weld interface are expressed by

Straight line A: When S ≦ 30 ppm

$$SEl = 107 - 220C_{eq}[FBW] \quad \cdots\cdots (6)$$

Straight line B: When S > 30 ppm

$$SEl = 77 - 154C_{eq}[FBW] \quad \cdots\cdots (7)$$

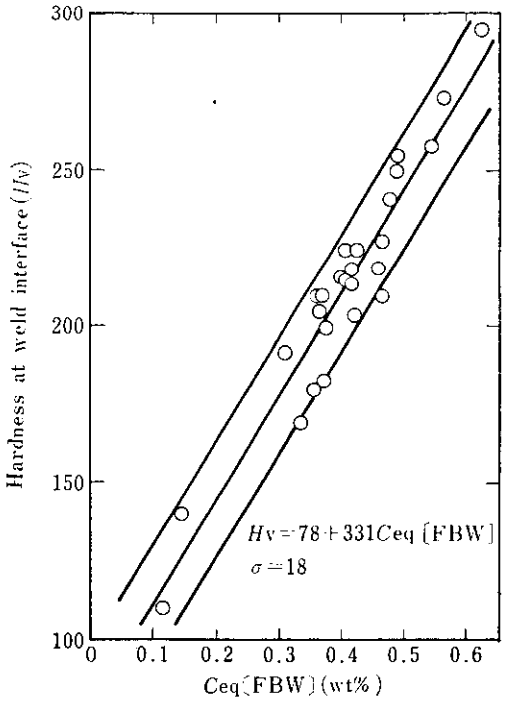

Fig. 7 Relation between hardness at weld interface and carbon equivalent, C_{eq}[FBW]

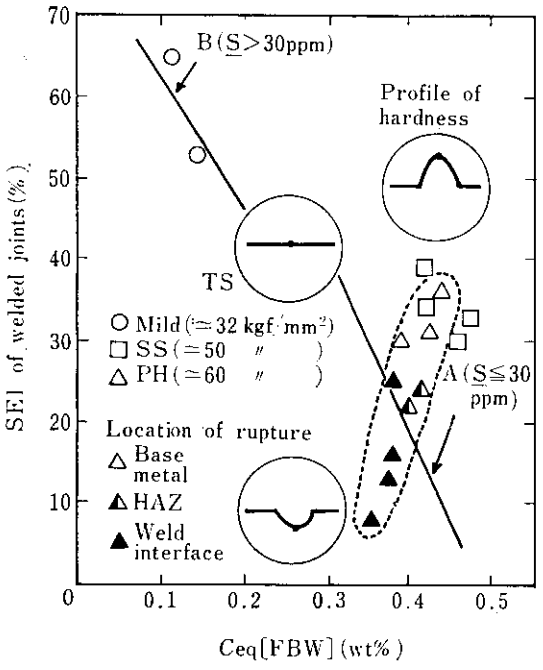

Fig. 8 Relation between SEI of welded joints and C_{eq} [FBW].

The positional relation between these two straight lines and the plotted values of various types of steel clearly indicates the features of the respective types of steel.

Both the S contents of the two types of mild steel (marked by ○) exceed 30 ppm, and these plotted values lie near straight line B. This is a logical result from the fact that the hardness of the sheet and that of the weld interface are nearly equal in mild steels, and as shown in **Fig. 4**, SEI of the welded joint hardly drops below that of the sheet.

The S contents of solid solution hardened steels (marked by □) having a TS value of about 50 kgf/mm² are all 30 ppm and under, and these plotted values are on the side where SEI values are higher than straight line A. This is due to the fact that the hardness of the weld interface of a solid solution hardened steel is higher than that of the base metal, so that deformation of the base metal occurs while the weld interface has not yet been deformed very much, and this was ascertained by measuring the intervals of the grids provided on the welded joint by electrolytic etching beforehand. Namely, a solid solution hardened steel containing a large quantity of solid solution hardening element such as Mn shows a higher value of C_{eq}[FBW], and SEI of the base metal governs that of the welded joint.

The S contents of precipitation hardened steels (marked by △, ▲ and ▲) having a TS value of about 60 kgf/mm² are all 30 ppm and under, and all these plotted values are distributed on both sides of straight line A. The SEI values of steels (marked by △) which have generated base-metal fracture are as high as 30% and over, and all the plotted values of SEI lie higher than straight line A. This is due to the fact that steels indicated by the △ mark have higher C_{eq}[FBW] values, as in the case of solid solution hardened steels (marked by □), and the SEI of the base metal governs that of the welded joint. Whereas in steels (marked by ▲) which have cracked at the weld interface, SEI values are as low as 25% and under, and lie exactly on the straight line A or on the side whose SEI value is lower than straight line A. This is due to the fact that the hardness of the weld interface of steels indicated by the ▲ mark is lower than that of the base metal, and thus deformation concentrated on the weld interface before the base metal became excessively deformed, and this fact has been ascertained by measuring the interval between the above-mentioned grids. Namely, steels indicated by the ▲ mark have lower C_{eq}[FBW], and the SEI value of the weld interface governs that of the welded joint, while the deformation range of the weld interface is very narrow compared with the entire welded joint, so that only SEI values which are lower than straight line A can be obtained. Two types of steel (marked by ▲) whose

SEl values are within the range of 20 to 25% have fractured at the HAZ, and their SEl values lie between straight line A and the group of steels which have cracked at base-metal (marked by △), but these hardness traverse are not flat in actuality, but resemble the hardness traverse of dual phase steel (see **Photo 3**). However, since the width of the softened zone is narrow and is separated from the weld interface by about 2 mm, such phenomenon appears, in any way, in precipitation hardened steels having an intermediate value of C_{eq}[FBW].

In the relation between SEl and C_{eq}[FBW] of the welded joint, crack modes are differentiated by eq. **(6)** as shown above, and it can be observed that the overall accuracy of the present experiment has been comparatively good. Judging from **Fig. 8**, it is necessary that in precipitation hardened steels having a TS value of about 60 kgf/mm², SEl of 30% or above cannot be obtained unless the C_{eq}[FBW] value is 0.4 wt% or more. The C_{eq}[FBW] values of precipitation hardened steels (I) and (II) mentioned earlier were 0.344 and 0.421 wt%, respectively, thereby indicating that the discussion thus far shows a good agreement with the empirical facts. Since TS of the sheet is affected by causes other than the chemical composition, no direct correspondence is found between C_{eq}[FBW] and TS of the sheet, and it is considered that the SEl value of the welded joint moves along the straight line A to the side of lower C_{eq}[FBW] for precipitation hardened steels having a TS value of about 50 kgf/mm² and to the side of higher C_{eq}[FBW] for the precipitation hardened steels of about 70 kgf/mm². Therefore, if precipitation hardened steels of about 50 kgf/mm² in TS are to be manufactured, no problem arises even if C_{eq}[FBW] is lower than 0.4 wt%, but if precipitation hardened steels higher in TS than 60 kgf/mm² are to be manufactured, a still higher C_{eq}[FBW] value would normally be required. As shown in **Fig. 3**, however, SEl of the sheet will become 25% and over when TS is 65 to 70 kgf/mm² and over, and thus the upper limit of TS for precipitation hardened steels to be used as material for making rims will have to be 65 to 70 kgf/mm².

Now, returning to the metallurgical meaning of C_{eq}[FBW] obtained by the multiple regression calculation, it may be said that the coefficients of respective elements in C_{eq}[FBW] indicate the degree of influence exercised upon the martensite or bainite transformation. In precipitation hardened steels, sheets are hardened by precipitates in addition to solid solution elements. Consequently, when the precipitates have dissolved during welding and precipitation does not occur sufficiently after welding, the weld softens. In order to prevent this, it is necessary to make the amount of structure hardening due to the martensite or bainite transformation larger than the amount of decrease in precipitation hardening, and for this purpose, the value of C_{eq}[FBW] must be increased. Since solid solution hardened steels have no such softening cause, no softening occurs. In other words, it can be said that steels which have been manufactured by making the strength of the sheet higher than the hardness, namely, the strength of the weld interface, are not suited as materials for making rims.

As shown in **Fig. 5**, the reasons for the variation in the penetrator cracking ratio due to the Mn/Si ratio are considered to be as follows: Elements composing the penetrator crack are Fe, Mn, Si, Al and others as mentioned earlier, but in the high strength steel sheets containing Mn of 0.9 wt% and over which were used in the present experiment, oxides of $MnO\text{-}SiO_2$ constitute the main ingredients. According to Yokoyama[8], in manufacturing pipes by ERW, the melting points of MnO and SiO_2 in the $MnO\text{-}SiO_2$ dual phase diagram are 1 850°C and 1 723°C, respectively, but when the Mn/Si ratio is within the range of 7 to 9, the melting point drops to the minimum value of about 1 250°C. The temperature at the melted zone at this time is estimated to be about 1 550°C. In flash butt welding, on the other hand, the temperature at the melted zone is estimated to be higher than 1 550°C[9]. As a result, it is considered that oxides of a steel whose Mn/Si ratio is wider than the range of 7 to 9 are also melted and discharged to the outside together with molten metal by the upset action. This fall in the penetrator cracking ratio when the Mn/Si ratio is within the range of as wide as 4 to 23 is considered to be attributable to the fact that in the manufacture of ERW pipes, there is no flashing and there are no oxides which have been generated are deposited, whereas in the manufacture of rims, oxides generated are removed continuously as they are generated by flashing.

The flash butt welded joints of precipitation hardened steels of TS about 60 kgf/mm², which have been commercially manufactured on the basis of the above-mentioned experimental results, have shown excellent cold formability.

5 Conclusion

Examination was made on the cold formability of hot rolled high strength sheet steels and their flash butt welded joints in relation to chemical composition and structure, and the following conclusions have been obtained:

(1) The side-bend elongation of the steel sheet drops as its tensile strength becomes higher. Even if tensile strength is equal, the sheet with samller S content shows greater side-bend elongation.
(2) Side-bend elongation of the flash butt welded

joint is smaller than that of the sheet. Particularly in the welded joint which has cracked at the weld interface or heat affected zone shows smaller side-bend elongation.

(3) The hardness traverse of the welded joint is heavily dependent on structual changes, and the crack position in the side-bend test coincides with the softened portion.

(4) Hardness H_V at the weld interface is dependent on the chemical composition of the sheet steel expressed by the carbon equivalent C_{eq}[FBW] which has been obtained by multiple regression calculations.

(5) Mild steel exhibits small differences in hardness and structure between the weld and base metal. Solid solution hardened steel and precipitation hardened steel which has a C_{eq}[FBW] of 0.4 wt% and over are hardened by the generation of martensite or bainite at the weld.

(6) Precipitation hardened steel having a C_{eq}[FBW] value of below 0.4 wt% does not generate martensite or bainite transformation at the weld, and causes a decrease in precipitation hardening, and thus becomes softer. Dual phase steel also softens, because its martensite is tempered by heat effect.

(7) In the dual phase steel and in precipitation hardened steel which has a C_{eq}[FBW] value of below 0.4 wt% and a TS value of about 60 kgf/mm², side-bend elongation of the welded joint is 25% and under, whereas in solid solution hardened steel and precipitation hardened steel which has a C_{eq}[FBW] value of 0.4 wt% and over and a TS value of about 60 kgf/mm², the side-bend elongation is within the range of 30 to 35%, which is larger than the 25% necessary for rim manufacture.

(8) The penetrator cracking ratio does not show a clear relation to Mn content and individual contents of other elements, but becomes the lowest when the Mn/Si ratio is within the range of 4 to 23.

(9) The hook cracking ratio becomes low when S content is 0.005 wt% and under.

References

1) S. Hashimoto, A. Kanbe and M. Sudoh: *Tetsu-to-Hagané*, **67** (1981) 4, S542
2) D. W. Dickinson: *Welding Design & Fabrication*, (1979) 5, p. 64
3) M. S. Rashid: Proceedings of Seminar "Dual Phase and Cold Pressing Vanadium Steels in the Automobile Industry", (1978), p. 32
4) M. S. Rashid and A. E. Rathke: SAE Paper, No. 810026
5) Y. Nakajima and C. Takita: Japan Patent No. 50–39583
6) F. S. Lepera: *J. Metals*, **32** (1980) 3, p. 38
7) G. T. Eldis and W. C. Hagel: Proceedings of Symposium "Hardenability Concepts with Applications to Steel", (1977), p. 397
8) E. Yokoyama: *Kawasaki Steel Technical Report*, **10** (1978) 1, p. 23 (in Japanese)
9) K. Ando, S. Nakata and I. Fukui: *Journal of the Japan Welding Society*, **40** (1971) 2, p. 137